Prediction of creep and stress-relaxation for cornea using fractional Maxwell model

Mohammadnabi Farrahi[1], Davood Domiri Ganji[1,*], Payam Jalili[2,3]

[1]*Department of Mechanical Engineering, Babol Noshirvani University of Technology, P.O. Box 484, Babol, Iran*

[2]*Department of Mechanical Engineering, NT.C., Islamic Azad University, Tehran, Iran*

[3]*Research Center for Modern Energy Technologies, North Tehran Branch, Islamic Azad University, Tehran, Iran*

*Corresponding Author: mirgang@nit.ac.ir

Keywords

Viscoelasticity;
Corneal biomechanics;
Creep test;
Stress-relaxation test.

Abstract

In this work, fractional calculus is used to model the viscoelastic behavior of the human cornea. The corneal response under simple stress conditions up to 5 MPa is described using a fractional-order Maxwell model. Two fractional parameters, α and β, are introduced to represent the stress–strain relationship, creep, and stress relaxation. The governing equation is transformed to the Laplace domain, and the time-domain response is recovered numerically by the Gaver–Stehfest method. The effects of α and β on the stress–strain, creep, and stress-relaxation responses are examined. At $\alpha = 0.8$ and $\beta = 0.6$, the model results closely agree with the experimental data. These calibrated parameters are then used to predict the creep and stress-relaxation behavior of the human cornea. The agreement between the predicted deformation and the experimental response supports the accuracy of the proposed model.

1 Introduction

As one of the most sensitive and important sensory organs in the human body, the eye has always been a subject of intense attention, and numerous studies have been conducted in the fields of biology and engineering to investigate it.

Boyce et al. [1] investigated the viscoelastic behavior of bovine cornea using uniaxial tensile and creep tests under load-controlled conditions. The results showed nonlinear time-dependent responses that could not be completely described by the quasi-linear viscoelastic model. Uchio et al. [2] conducted simulations and experiments on the human cornea, primarily focusing on determining the mechanical and physical conditions of impact by foreign objects, which often lead to intraocular foreign body (IOFB) injuries. Another study by Friberg and Lace [3] also demonstrated that the human cornea exhibits similar responses in wet laboratory tests. The common viscoelastic models include the classical Kelvin-Voigt, Maxwell, and standard linear solid models. In recent years, structural equations employing fractional calculus for viscoelastic materials have gained significant attention as they require fewer parameters to describe the viscoelastic behavior of materials than traditional models. Previous research has reported a wide range of Young's modulus, varying from 0.159 MPa to 57 MPa, and has also stated that corneal tissue has a viscosity coefficient of 9.02 kPa·s and an elastic modulus of 11.05 MPa [3, 4]. Ávila et al. [5] conducted a comprehensive experimental study on the biomechanical and optical properties of the living human cornea using the Standard Linear Solid Model (SLSM). Their results showed that separating the elastic and viscous components of corneal response provides a more accurate assessment of viscoelastic behavior than global indices such as corneal hysteresis, and helps clarify the influence of intraocular pressure on corneal elasticity and viscosity. In a study, Kampmeier et al. [6] examined the physical properties of porcine corneas to enhance corneal modeling accuracy in refractive surgery. Their findings confirmed the cornea's viscoelastic nature and reported directional stiffness differences between the inferior–superior and nasal–temporal axes. Downs et al. [7] examined viscoelastic changes in scleral tissues during the early stages of glaucoma, revealing that intraocular pressure can alter the biomechanical properties of ocular tissues. Hosseini-Farid et al. [8] investigated stress-relaxation in biological soft tissues using quasi-linear viscoelastic (QLV) theory and found that immediate stresses were more than ten times higher than equilibrium stresses, confirming the time-dependent nature of soft tissue behavior. Ahmadi Nejad et al. [9] developed a numerical model to study the mechanical response of neural cells under blast loading using viscoelastic material assumptions. Their results showed that the presence of microtubule networks reduced overall displacement and von Mises stress by about 50%. In another study, Merlini [10] simulated the transient elastographic response of the cornea using a stabilized Leapfrog method based on Chebyshev polynomials. By incorporating anisotropic and hyperelastic properties into a 3D corneal model under intraocular pressure, they proposed a reliable computational framework for real-time, non-invasive corneal diagnostics.

Badawy et al. [11] explored bioengineered corneal substitutes using plant-based materials to address donor shortages, evaluating mechanical, optical, and biocompatibility properties of crosslinked protein structures. Elsheikh et al. and Zeng et al. [12, 13] conducted comparative experiments to investigate the biomechanical and viscoelastic properties of human and porcine corneas. Under swelling and tensile loading, they evaluated stress–strain relationships, creep, and stress-relaxation behaviors. The results revealed that while both corneas exhibited similar short-term responses, human corneas were significantly stiffer and showed lower long-term creep and slower stress-relaxation compared with porcine corneas. These findings highlight the greater structural integrity and resistance of human corneas to time-dependent deformation. Wang et al. [14] developed a nonlinear viscoelastic constitutive model based on fractional derivatives to describe the ratcheting response of polymers under time- and historydependent loading conditions. The model, formulated within a fractional Poynting–Thomson framework, accurately captured experimental results while requiring only nine physically meaningful parameters, demonstrating the efficiency and predictive power of fractional-order approaches compared with classical models. Ilić et al. [15] experimentally measured the elastic modulus of blood vessels by analyzing balloon inflation in interventional radiology procedures. Their analytical model successfully related pressure–volume data to tissue elasticity, demonstrating the applicability of mechanical testing methods in soft biological tissues. In another study, Nguyen et al. [16] proposed a structural model to describe the nonlinear and anisotropic viscoelastic behavior of the corneal stroma. By averaging the elastic and viscous responses of individual lamellae, their model incorporated the cornea's lamellar microstructure into the constitutive formulation and accurately predicted nonlinear stress–strain and creep behaviors under cyclic loading. Mandal et al. employed fractional calculus to model the viscoelastic behavior of the human cornea, demonstrating that fractional parameters effectively describe both elasticity and viscosity. They applied fractional Maxwell and Kelvin-Voigt models for stress levels up to 250 MPa and obtained analytical solutions of the equations using the Laplace transform method. The results indicated that the fractional Maxwell model converges to the classical model for specific parameter values, accurately representing the cornea's stress–strain relationship [17]. Das et al. [18] proposed a fractional Kelvin–Voigt model (FKVM) to describe the viscoelastic response of single biological cells and validated its accuracy across multiple timescales. The study demonstrated that the fractional parameters α and β effectively represent viscous damping and elastic recovery, respectively, allowing compact yet accurate prediction of creep, recovery, and relaxation behaviors in soft biological tissues. In a related study, Taheran et al [19] analyzed the dynamic response of a viscoelastic microcantilever beam using a modified strain gradient theory. By combining the Kelvin–Voigt model with Hamilton's principle and applying the Galerkin method, they demonstrated that scale effects and nonlinear parameters significantly influence the dynamic behavior and natural frequency of microsystems. Building on previous corneal biomechanics studies, Glass et al. [20] investigated how variations in elasticity and viscosity influence corneal hysteresis. Using a MATLAB-based three-element spring–damper model, they demonstrated that increasing the stiffness of the viscoelastic element reduces hysteresis, whereas increasing the stiffness of the purely elastic element amplifies it. Their findings emphasize the interplay between elastic and viscous components in determining the cornea's time-dependent mechanical response, aligning well with clinical observations.

Pang et al. [21] reviewed finite-element modeling of the human cornea, with particular attention to geometric reconstruction, constitutive formulations, and future developments in computational corneal biomechanics. In a comprehensive study, Song et al. [22] examined the viscoelastic properties of posterior ocular tissues, including the optic nerve, its sheath, and the sclera, using creep tests on postmortem human eyes. Their analysis, based on the Prony series and Deborah number evaluation, revealed that all tissues followed linear viscoelastic behavior, with the optic nerve showing the highest compliance and the sclera the lowest. These results confirmed the time-dependent mechanical nature of ocular tissues and underscored the importance of viscoelastic modeling in understanding the biomechanics of the eye. Lopes et al. [23] reviewed recent technological advances in in-vivo corneal biomechanics assessment. They discussed the evolution of diagnostic devices, such as the Ocular Response Analyzer (ORA) and Corvis ST, noting that newer parameters, like the stress–strain index, have improved the estimation of corneal elastic modulus under different intraocular pressures. Additionally, recent progress in Brillouin microscopy has enabled the development of clinically compatible instruments, marking a significant step toward the precise and non-invasive measurement of corneal biomechanical properties. Bettahar et al. [24] analyzed the biomechanical consequences of eye rubbing in keratoconus patients using clinical data and numerical simulations. Their results revealed that repetitive eye rubbing induces corneal deformation and local stress elevation, particularly in advanced stages of the disease, underscoring the mechanical contribution of external loading to corneal weakening and degeneration.

The concept of fractional calculus was first introduced by Nutting [25] who described stress-relaxation behavior using non-integer powers of time rather than conventional exponential functions. Later, Scott-Blair [26] expanded on Nutting's work by applying fractional derivatives to model the rheological properties of viscoelastic materials such as rubber and polymers, laying the foundation for modern fractional viscoelastic theory. Expanding the practical applications of fractional viscoelastic theory, Makris et al. [27] developed a fractional Maxwell model for viscoelastic dampers used in vibration isolation systems. Their model was validated through dynamic experiments, showing excellent agreement with both analytical predictions and measured responses. The study also introduced numerical algorithms to solve the constitutive equations in both the frequency and time domains, confirming the robustness and computational efficiency of the fractional Maxwell approach. Building on earlier theoretical work, Lewandowski et al. [28] developed parameter identification techniques for fractional Kelvin–Voigt and Maxwell models by analyzing hysteresis curve characteristics. Their approach successfully extracted model parameters from both simulated and experimental datasets, demonstrating the accuracy and reliability of fractional viscoelastic formulations for real-world materials. Recent analytical advances in fractional differential equations, such as those by Almuneef and Hagag [29], have demonstrated the flexibility and effectiveness of fractional calculus in solving complex physical systems, further supporting its use in viscoelastic modeling. Tan et al. [30] applied fractional calculus to derive the constitutive relationships of viscoelastic fluids and demonstrated that fractional orders strongly affect flow-field behavior. Their results showed that increasing the fractional order reduces the viscoelastic influence on shear stress over time, revealing the inherent memory and time-dependent nature of such materials. Qi and Jin [31] investigated unsteady flow behavior in viscoelastic fluids using the fractional Maxwell model. By applying the Laplace and limited cosine Fourier transforms, they obtained exact analytical solutions for specific pressure-gradient cases, demonstrating the mathematical robustness of the fractional Maxwell formulation in modeling time-dependent viscoelastic systems. Extending the application of the fractional Maxwell model to dynamic flow analyses, Yin et al. [32] and Jia et al. [33] investigated oscillatory viscoelastic flows under varying frequency conditions. Their analytical solutions in both time and frequency domains demonstrated that fractional parameters significantly modify resonance peaks, velocity amplitudes, and even flow direction. These findings reveal the critical influence of fractional orders on the nonlinear and frequency-dependent behavior of viscoelastic systems, underscoring the model's ability to capture complex time-dependent responses. Tripathi [34] investigated sinusoidal oscillatory flow of viscoelastic fluids using the fractional Maxwell model and analytical methods such as the Homotopy Perturbation and Adomian Decomposition techniques to evaluate the influence of fractional parameters on pressure and friction. Tripathi et al. [35] analyzed peristaltic transport of fractional Maxwell fluids in coaxial tubes under endoscopic conditions, reporting that pressure decreases with increasing fractional parameters while frictional forces in the inner and outer tubes act in opposite directions. Nguedjio et al. [36] applied a Zener-type fractional model to tropical wood, achieving over 95% accuracy in creep–recovery predictions and enhancing model performance through the inclusion of nonlinearity and stress-dependent parameters. Abukhaled and Abukhaled [37] employed the residual power series method to solve the fractional anisotropic curvature equation of the cornea, producing an explicit curvature profile that was validated against both integer and fractional solutions for diagnostic use. In parallel, Arif et al. [38] proposed a stochastic numerical framework for non-Newtonian nanofluid flow under the influence of both magnetic and chemical forces, providing reliable insights into the multiparametric viscoelastic behavior. Ciancio et al. [39] coupled fractional calculus with nonequilibrium thermodynamics to model energy dissipation and relaxation in viscoelastic media. Zheng et al. [40] extended fractional modeling using the Caputo–Fabrizio derivative for magnetohydrodynamic electroosmotic flow, where larger fractional parameters induced oscillatory responses and non-classical. Bonifasi Lista et al. [41] observed nonlinear viscoelastic behavior in human soft tissues, where applied stress influenced both creep and stress-relaxation rates, suggesting partial viscoelastic activity. Shah et al. [42] developed analytical Laplace–Weber solutions for Poiseuille and Couette flows, providing a theoretical basis for modeling time-dependent viscous effects. Friedrich [43] introduced a four-parameter fractional Maxwell model using Riemann–Liouville derivatives, which accurately reproduced viscoelastic stress–strain responses. Building on these studies, the present work applies the fractional Maxwell model with Laplace transformation in MATLAB to analyze the human cornea, determine optimal fractional coefficients, and predict creep and stress-relaxation phenomena. Understanding time-dependent mechanical behavior is essential for accurately predicting long-term deformation in complex materials, as demonstrated in recent studies exploring creep evolution and stress-dependent deformation mechanisms in advanced engineering composites and high-performance concrete materials [44-46]. Recent research has also highlighted the value of advanced modeling strategies and specially designed mechanical systems capable of capturing nonlinear or customized force responses, which offer new opportunities for describing complex viscoelastic behavior [47-48].

This study develops a fractional Maxwell model (FMM) combined with Laplace transformation and Stehfest numerical inversion to describe the creep and stress-relaxation behavior of the human cornea. The model incorporates the Caputo fractional derivative to represent time-dependent and memory effects, governed by two fractional parameters (α and β) corresponding to viscous damping and elastic recovery. Model parameters were calibrated using experimental stress–strain data reported in the literature, and the predictions were evaluated for both creep and stress-relaxation responses. The Laplace–Stehfest numerical inversion was employed instead of the analytical Mittag–Leffler formulation, as it provides a more stable and practical approach for handling multi-parameter fractional systems and experimental datasets, thereby avoiding the convergence and computational difficulties associated with Mittag–Leffler evaluations. Overall, this work employs a fractional viscoelastic formulation in corneal biomechanics to offer a physically interpretable and computationally efficient framework for characterizing the time-dependent mechanical response of ocular tissue.

2 Mathematical model

2.1 Maxwell model [49]

A linear elastic spring and a linear viscous dashpot can be used to create rheological models. The Maxwell model and Kelvin-Voigt model are examples of such models. The Maxwell model is the simplest and one of the earliest viscoelastic models, consisting of a spring and a dashpot arranged in series (Fig. 1). The governing equation for this model is as follows.

$$\sigma + \frac{\eta}{E}\dot{\sigma} = \eta\dot{\varepsilon} \tag{1}$$

2.2 Creep-recovery response of the Maxwell model

Physically, when the Maxwell model is subjected to a stress σ_0, the spring stretches instantly while the damper requires time to respond. Upon removing the load, the spring reacts quickly, but the damper shows little inclination to recover. Therefore, immediate elastic recovery occurs while the creep strain caused by the damper remains. The complete creep and recovery response is illustrated in Fig. 2.

2.3 Fractional Maxwell model

The following equation describes the constitutive relation of the fractional Maxwell model

$$\sigma(t)+\lambda^{\alpha}\frac{d^{\alpha}\varepsilon(t)}{d^{\alpha}t}=\mu\lambda^{\beta}\frac{d^{\beta}\varepsilon(t)}{d^{\beta}t} \tag{2}$$

Here η is the constant viscosity coefficient, μ is the shear modulus, $\lambda = \frac{\eta}{\mu}$ is the relaxation time, σ is the shear stress, ε is the shear strain, and α, β are fractional parameters that fulfill $0 < \alpha, \beta < 1$.

Moreover, the stress–strain relationship of fractional derivative order is obtained from the following equation.

$$\sigma(t)=\mu\lambda^{\gamma}\left(\frac{d^{\gamma}\varepsilon(t)}{d^{\gamma}t}\right) \tag{3}$$

When $\gamma = 0$, a particular example of this model is inferred that illustrates the behavior of a completely elastic element and leads to Hooke's Law. Conversely, the example of a fully viscous element represented by the Newtonian Law may be inferred by setting $\gamma = 1$. Therefore, the previously mentioned model can be seen as a realistic model that falls between these two ideal and typical scenarios.

A fractional element obeying the aforementioned equation is inserted to build the fractional model (Fig. 3). This fractional element is represented by a triangle (Fig. 3(c)) and is determined by three parameters: γ, μ, λ. Moreover, the fractional element is regarded as a part of viscoelastic models, much as the spring and damper shown in sections (a) and (b).

In this study, the Caputo fractional derivative is adopted to describe the behavior of the fractional element and capture the hereditary, time-dependent response of the corneal tissue. The Caputo definition is particularly advantageous for viscoelastic modeling because it allows the use of physically interpretable and experimentally measurable initial conditions (in terms of stress and strain), unlike the Riemann–Liouville formulation that requires non-physical fractional initial values. Mathematically, the Caputo operator interchanges the order of differentiation and integration, producing finite, physically realistic initial conditions while maintaining dimensional consistency between integer- and fractional-order terms. These properties ensure both mathematical compatibility with Laplace transform techniques and the physical interpretability of the model, making the Caputo definition the most suitable choice for simulating time-dependent deformation in biological soft tissues, such as the cornea.

Fig. 4 displays the fractional Maxwell and classical models. The fractional elements are shown in part (b) based on the generalized stress–strain relationship.

$$\begin{aligned}\sigma_1(t)&=\mu_1\lambda_1^{\gamma_1}\frac{d^{\gamma_1}\varepsilon_1}{dt^{\gamma_1}}\\ \sigma_2(t)&=\mu_2\lambda_2^{\gamma_2}\frac{d^{\gamma_2}\varepsilon_2}{dt^{\gamma_2}}\end{aligned} \tag{4}$$

Because the components are connected in series [50],

$$\sigma(t)+\lambda^{\gamma_1-\gamma_2}\frac{d^{\gamma_1-\gamma_2}\sigma(t)}{dt^{\gamma_1-\gamma_2}}=\mu\lambda^{\gamma_1}\frac{d^{\gamma_1}\varepsilon(t)}{dt^{\gamma_1}} \tag{5}$$

Eq. (5) thus represents the constitutive governing Eq. of the fractional Maxwell model. By substituting $\gamma_1 - \gamma_2$ and γ_1 with α and β, respectively, Eq. (2) simplifies to Eq. (1), where the two fractional parameters take the forms $\alpha = |\gamma_1 - \gamma_2|$ and $\beta = \max\{\gamma_1, \gamma_2\}$.

By applying the Laplace transform to Eq. (2) and incorporating the initial conditions, i.e., $t = 0\,;\ \sigma(0) = \varepsilon(0) = 0$ indicates that no deformation occurs when no force is applied. Moreover, by simultaneously using the Laplace transform of Caputo fractional derivative (Eq. (6)), we obtain:

$$s^{\alpha}F(s)-\sum_{k=0}^{n-1}s^{\alpha-k-1}f^{(k)}(0), n-1\le\alpha<n \tag{6}$$

$$L\left\{\sigma(t)+\lambda^{\alpha}\frac{d^{\alpha}\varepsilon(t)}{d^{\alpha}t}\right\}=L\left\{\mu\lambda^{\beta}\frac{d^{\beta}\varepsilon(t)}{d^{\beta}t}\right\}$$

$$\sigma(s)+\lambda^{\alpha}s^{\alpha}\sigma(s)-\lambda^{\alpha}\sum_{k=0}^{\alpha}s^{\alpha-1}\sigma^{(k-1)}(0)=\mu s^{\beta}\varepsilon(s)-\mu\sum_{k=0}^{\alpha}s^{\beta-1}\sigma^{(k-1)}(0) \tag{7}$$

$$\sigma(s)+\lambda^{\alpha}s^{\alpha}\sigma(s)=\mu s^{\beta}\varepsilon(s)$$

Applying these steps yields Eq. (8), which is used to obtain the creep and stress-relaxation responses in MATLAB. Because the inverse Laplace transform is difficult to evaluate directly, the Gaver-Stehfest method is used for numerical inversion.

$$\sigma(s)=\varepsilon(s)\frac{\mu s^{\beta}}{(1+\lambda^{\alpha}s^{\alpha})}$$

$$\varepsilon(s)=\frac{\sigma(s)}{\mu\left[\frac{1}{s^{\beta}}+\lambda^{\alpha}s^{\alpha-\beta}\right]} \tag{8}$$

2.4 *The Gaver-Stehfest method*

Since Eq. (6) typically lacks an analytical inverse Laplace transform and cannot be solved directly, we employed the Stehfest numerical method for its computation. This method is recognized as a reliable and effective tool for analyzing fractional differential equations and simulating material behavior in continuous media, due to its high precision and ability to accurately reproduce time functions from the Laplace domain. Introduced in the late 1960s, the Stehfest method approximates the time domain solution as follows,

$$f(t)=\frac{\ln 2}{t}\sum_{K=1}^{N}V_K.F(K.\frac{\ln 2}{t}) \tag{9}$$

where V_k is given by

$$V_K=(-1)^{K+\frac{N}{2}}\sum_{j=\frac{K+1}{2}}^{\min(K,\frac{N}{2})}\frac{j^{\frac{N}{2}}(2j)!}{(\frac{N}{2}-j)!\,j!(j-2)!(k-j)!(2j-k)!} \tag{10}$$

The parameter N in Eq. (7) indicates the number of terms used and must be even, typically determined through trial and error. The method's accuracy is significantly influenced by N; initially, increasing N enhances accuracy, but rounding errors can reduce precision beyond a certain point. Researchers have proposed various optimal values for N, with Cheng and Sidauruk recommending that it ideally be between 6 and 20[51]. Although analytical solutions of fractional differential equations can be expressed through the Mittag–Leffler (MLF) function, such approaches are often computationally intensive and prone to convergence difficulties, particularly when dealing with multi-parameter viscoelastic models or experimental datasets. In contrast, the Laplace–Stehfest numerical inversion method offers a stable and efficient alternative, enabling the direct recovery of time-domain responses from Laplace-domain formulations without the need for explicit evaluation of special functions. This method enables accurate and robust computation of creep and stress-relaxation curves for fractional-order systems, while offering controllable numerical precision through the selection of the term number N in the inversion process. Modeling viscoelastic materials using the fractional Maxwell model requires only two fractional parameters, α and β. These coefficients were calculated and compared for the cornea, for which the experimental stress–strain curve is available, to determine the optimal values for stress-time and strain-time curves. For this purpose, the best coefficients were extracted using MATLAB, and the results were obtained. We set the fractional parameters equal to one (which converges to the classical Maxwell model) to validate these findings from the stress-time and strain-time curves. We compared the results with modeling a viscoelastic material with corneal properties in Abaqus software.

Table 1 summarizes the complete Gaver-Stehfest numerical inversion procedure used to recover the time-domain response of the fractional Maxwell model from its Laplace-domain formulation.

3 Validation

As mentioned earlier, Eq. (6) does not have an analytical inverse Laplace transform; therefore, we used the Gaver-Stehfest method for the inverse Laplace calculation. To verify the accuracy of this method, we tested it on the specific function $\frac{1}{s+1}$, for which an analytical inverse Laplace transform is available, and evaluated the numerical precision. The results demonstrate the accuracy of this method, as shown in Fig. 5. Since the results from testing the Stehfest method were fully validated and acceptable, we can confidently use this method to obtain our desired results.

To validate the stress-relaxation and creep tests, we simulated a corneal element with properties described in the literature using the Abaqus software under simple tension and the Maxwell behavioral model. The properties used were as follows: viscosity of 9.02 KPa. s, elastic modulus of 11.05 MPa (corneal elastic limit), stress-relaxation time of 0.002318 seconds, Poisson's ratio of 0.422, applied stress of 500 kPa, and test duration of 50 seconds. After completing the simulation, we compared the results from this analysis with those obtained from the developed code. The applied loading and boundary conditions for both phenomena are shown in Fig. 6.

Figures 7 and 8 show a strong overlap between the creep and stress-relaxation test results (with α and β set to one, matching the classical Maxwell model) and the cornea simulations in Abaqus. This alignment confirms the accuracy and reliability of the developed code, demonstrating its effectiveness in simulating the mechanical properties of the human cornea, which is consistent with the results obtained using Abaqus.

The fractional parameters α and β also have physiological relevance in the context of corneal biomechanics. The parameter **α** reflects the level of viscous damping within the tissue and thus describes how rapidly the cornea dissipates mechanical energy during deformation. Higher α values are associated with stronger time-dependent resistance to flow, a behavior typically observed in softer or more hydrated stromal lamellae. In contrast, the parameter **β** represents the elastic recovery component and governs the stiffness of the collagen microstructure. Larger β values correspond to a more pronounced elastic response and faster recoil after unloading, which is consistent with tighter collagen packing. Together, α and β interpolate between the viscous and elastic limits, enabling the model to reproduce the combined, physiologically realistic viscoelastic response of the cornea.

4 Stress-strain curves

The main goal is to find the optimal α and β coefficients that best fit the experimental stress–strain curve for the cornea. Using MATLAB and Eq. (8), various combinations of these coefficients are tested, and the results are compared with experimental data to minimize error and achieve the best match (Fig. 9). Once the optimal values are identified, they are used to generate stress-relaxation and creep curves, which help understand the cornea's biomechanical and viscoelastic behavior. This process optimizes the model for predicting corneal behavior under different conditions.

A comprehensive comparison between the experimental data, Abaqus simulation, and the classical Maxwell model ($\alpha = \beta = 1$) highlights the effectiveness of the methods used in this research. As shown in Fig. 10, this comparison validates the accuracy of the results and emphasizes the value of the proposed models in simulating the mechanical behavior of the cornea.

4.1 Observation of the stress–strain curves

The first set of observations was obtained by numerically inverting the Laplace-domain governing equation for each combination of fractional parameters over the experimental stress range.

Stress-strain curves for various combinations of fractional parameters were generated and thoroughly compared with experimental data from studies on human cornea and sclera to assess the accuracy and alignment of the current theoretical model. These curves, derived after calculating values using the inverse Laplace transform of the governing equation, were adjusted for specific parameter values and compared in detail with the findings of Friberg and Lace, as shown in Fig. 9(a–f).

The values of $\alpha = 0.8$ and $\beta = 0.6$, the theoretical results closely align with the experimental data. However, when α is reduced to 0.2, the deviation between the theoretical and experimental data peaks. Among all combinations of fractional parameters α and β, Fig. 9(a) shows the greatest discrepancy with experimental data. The minimum and maximum deviations occur at the lowest and highest stress levels, measuring 0.052 and 0.13, respectively. As seen in Figures 9(a)–(f), the smallest differences between theoretical and experimental results occur for $\alpha = 0.8$ and $\beta = 0.6$.

Fig. 10 presents the stress–strain curve for fractional parameters $\alpha = 0.8$ and $\beta = 0.6$, showing a notably good agreement with the experimental results. For specific stress values, the calculated theoretical strain aligns well with the experimental data from scientific sources (experimental studies suggest that corneal tissue failure occurs at 18% strain).

Fig. 10 also presents the stress–strain curve for the traditional Maxwell model, which can be derived by setting the fractional parameters α and β to 1. In the governing equation of the fractional Maxwell model, when α and β are set to 1, the equation naturally converts to that of the classical Maxwell model. A significant difference is observed between the mathematical behavior obtained and the experimental results reported by Friberg in the stress–strain curve (in this case, the maximum strain for the classical model was recorded as 0.042).

Overall, it can be concluded that the deformation values obtained from mathematical calculations show a strong resemblance to the experimental results, with a maximum strain of approximately 14.1% or 0.141 mm/mm. Based on this outcome, the corneal tissue can be modeled using the fractional Maxwell model to preserve the characteristics of the actual material behavior curve. Therefore, the precise selection of fractional parameters in the Maxwell model enables accurate and realistic mathematical modeling of the cornea and human tissue.

4.2 *Stress relaxation and creep of the cornea*

Now that we have determined the optimal parameters, we can confidently predict the stress-relaxation and creep curves for the cornea. By substituting the optimized values of α and β into the current model, we obtain the corneal stress-relaxation (Fig. 11.) and creep (Fig. 12.) curves.

5 Sensitivity analysis on α and β

As observed in the previous section, variations in the α and β parameters significantly impact the material's behavior. For this reason, a sensitivity analysis has been conducted on these parameters for stress-relaxation and creep phenomena to examine the effects of these changes more precisely. The fractional parameters α and β also have physiological relevance in the context of corneal biomechanics. The parameter α reflects the level of viscous damping within the tissue and thus describes how rapidly the cornea dissipates mechanical energy during deformation. Higher α values are associated with stronger time-dependent resistance to flow, a behavior typically observed in softer or more hydrated stromal lamellae. In contrast, the parameter β represents the elastic recovery component and governs the stiffness of the collagen microstructure. Larger β values correspond to a more pronounced elastic response and faster recoil after unloading, which is consistent with tighter collagen packing. Together, α and β interpolate between viscous and elastic limits and enable the model to reproduce the combined, physiologically realistic viscoelastic response of the cornea.

The fractional parameter values used throughout the sensitivity analyses are summarized in Table 2.

5.1 *Stress relaxation: fixed α and variable β (Fig. 13)*

5.2 *Effect of fixed α on stress-relaxation*

At the start of this experiment, when the time is zero, the stress is at its maximum value. This peak stress gradually decreases over time and eventually reaches a constant value. This behavior aligns precisely with stress-relaxation characteristics, where the stress in a material decreases over time under a constant strain (Fig. 13).

When the value of α is kept constant at 0.2, it is observed that as β increases from 0.2 to 0.6, the peak stress values gradually rise, reaching a maximum at $\beta = 0.6$. Beyond this point, further increases in β lead to a decrease in peak stress values. Therefore, $\beta = 0.6$ is considered the peak point for maximum stress values. This pattern of change repeats for all values of α, except when α and β are equal to 1, representing the behavior of the classical Maxwell model. This model exhibits simpler behavior without the complex variations seen in fractional values.

Regarding the minimum stress values, the results are also noticeable. As β increases, for constant values of α, the minimum stress values also continuously rise. This increase follows an upward trend, where the slope of the graph for minimum stress changes becomes steeper as β increases.

5.3 *Stress relaxation: fixed β and variable α (Fig. 14)*

5.4 *Effect of fixed β on stress-relaxation*

As shown in Fig. 14, in terms of initial stresses in the stress-relaxation test, an increase in the value of α results in a nearly linear increase in stress at the beginning of the test. Specifically, when β is held constant, the initial stress values significantly rise with an increase in α; however, after α reaches 0.6, this upward trend gradually levels off. This pattern is consistent across all constant β values and varying α.

In contrast, regarding the final stresses of this test, it is observed that increasing the α values around β = 0.5 does not affect the final stress values; in other words, within this range, the final stresses show little sensitivity to changes in α. Additionally, as the value of β increases, the overall slope of the graph decreases. This decrease in slope indicates that the β parameter significantly impacts the slope variations of the graphs and can influence the material's behavior. This highlights the critical importance of accurately adjusting the fractional parameters in mechanical models.

5.5 *Creep: fixed α and variable β (Fig. 15)*

5.6 *Effect of fixed α on creep*

In the creep test, the material's creep behavior is such that at time zero, the strain is also zero due to the zero stress. However, while the stress is kept constant over time, the strain gradually increases until it reaches a specific value and stabilizes. This behavior precisely defines the phenomenon of creep. Therefore, the initial (minimum) strain values for all cases of α and β will be zero, in contrast to the stress-relaxation test.

Regarding the maximum strain values, the pattern is different. When α is kept constant, the strain increases as β rises. This upward trend continues until β reaches 0.8, after which the strain values decrease. Thus, β =0.8 represents the peak or maximum strain in this case. These results are clearly shown in Fig. 15.

5.7 Creep: fixed β and variable α (Fig. 16)

5.8 Effect of fixed β on creep

As previously mentioned, it is evident that at time zero, meaning at the beginning of the creep test, the strain value is also zero. Therefore, there is no discussion regarding the initial values, as all values are zero. However, concerning the final values, it can be observed that as the value of α increases, while keeping β constant, the final values also increase. This increase continues up to α = 0.5, after which the values tend to decrease or converge to a constant value.

On the other hand, increasing the value of β significantly impacts the rate of change of these values, such that as the value of β increases, the rate of change also rises. This highlights the direct and meaningful influence of the parameters α and β on the creep behavior of the material (Fig. 16).

6 Discussion

Compared with conventional integer-order models, fractional constitutive equations can represent viscoelastic behavior with fewer parameters while retaining the material's memory effects. Previous studies have shown that appropriate selection of fractional parameters can substantially improve agreement between experimental data and theoretical predictions. The Caputo derivative is especially useful in biomechanical applications because it accommodates physically interpretable initial conditions. Related corneal-shape analyses have also demonstrated the effectiveness of fractional boundary-value formulations and least-squares solution techniques [52].

Fractional-order derivatives have also been used to describe neuronal firing and the influence of self-similar dendritic structures. Guo et al. [53] related fractional spiking behavior to recursively organized resistor-capacitor networks representing smooth and spiny dendrites, illustrating the broader ability of fractional temporal operators to capture memory and scale-dependent responses in biological systems.

The present study extends the conventional Maxwell model by replacing integer-order stress-strain derivatives with fractional derivatives. After transformation to the Laplace domain, the Gaver-Stehfest method is used to recover the time-domain strain and stress responses for different values of α and β. The resulting stress-strain, creep, and stress-relaxation curves demonstrate that the human cornea behaves between the ideal elastic and viscous limits. The close agreement with experimental data indicates that the fractional Maxwell formulation provides a compact and physically interpretable representation of the cornea's time-dependent viscoelastic response.

7 Conclusions

This study has successfully modeled the stress-relaxation and creep behavior of the human cornea using the fractional Maxwell model, precisely refining the values of the involved parameters. The final calibrated values are $\alpha = 0.8$ and $\beta = 0.6$. In this model, a purely viscous component is represented by a value of 0, while a perfectly elastic component has a value of 1. Consequently, the constitutive model displays a nonlinear viscoelastic response for the tissue. Examining the deformation type, creep, and stress-relaxation offers a clear perspective on the model's accuracy. It was observed that the fractional Maxwell model shows strong alignment with experimental data derived from human samples.

Beyond its numerical performance, the fractional Maxwell formulation also offers potential relevance for biomechanical assessments of the cornea. By characterizing the time-dependent mechanical response, the model may contribute to a better understanding of corneal stability under physiological loading. Accordingly, the proposed framework provides a useful basis for future clinical or diagnostic developments in corneal biomechanics.

References

1. Boyce, B.L., Jones, R.E., Nguyen, T.D., et al. "Stress-controlled viscoelastic tensile response of bovine cornea", *Journal of Biomechanics*, 40(11), pp. 2367-2376 (2007). https://doi.org/10.1016/j.jbiomech.2006.12.001
2. Uchio, E., Ohno, S., Kudoh, J., et al. "Simulation model of an eyeball based on finite element analysis on a supercomputer", *British Journal of Ophthalmology*, 83(10), pp. 1106-1111 (1999). https://doi.org/10.1136/bjo.83.10.1106
3. Andreassen, T.T., Simonsen, A.H., and Oxlund, H. "Biomechanical properties of keratoconus and normal corneas", *Experimental Eye Research*, 31(4), pp. 435-441 (1980). https://doi.org/10.1016/S0014-4835(80)80027-3
4. Elsheikh, A., Wang, D., Brown, M., et al. "Assessment of corneal biomechanical properties and their variation with age", *Current Eye Research*, 32(1), pp. 11-19 (2007). https://doi.org/10.1080/02713680601077145
5. Ávila, F.J., del Barco, Ó., Marcellán, M.C., et al. "A comprehensive study on elasticity and viscosity in biomechanics and optical properties of the living human cornea", *Photonics*, 11(6), Art. 524 (2024). https://doi.org/10.3390/photonics11060524
6. Kampmeier, J., Radt, B., Birngruber, R., et al. "Thermal and biomechanical parameters of porcine cornea", *Cornea*, 19(3), pp. 355-363 (2000). https://doi.org/10.1097/00003226-200005000-00020
7. Downs, J.C., Suh, J.K.F., Thomas, K.A., et al. "Viscoelastic material properties of the peripapillary sclera in normal and early-glaucoma monkey eyes", *Investigative Ophthalmology & Visual Science*, 46(2), pp. 540-546 (2005). https://doi.org/10.1167/iovs.04-0114
8. Hosseini-Farid, M., Rezaei, A., Eslaminejad, A., et al. "Instantaneous and equilibrium responses of the brain tissue by stress relaxation and quasi-linear viscoelasticity theory", *Scientia Iranica*, 26(4), pp. 2047-2056 (2019). https://doi.org/10.24200/sci.2019.21314
9. Ahmadi Nejad Joushani, H., Vahidi, B., and Sabour, M.-H. "Numerical simulation of a neuron under blast load using viscoelastic material models", *Scientia Iranica*, 28(1), pp. 255-264 (2021). https://doi.org/10.24200/sci.2019.51975.2456
10. Merlini, G. *Mechanical and numerical modelling of transient shear wave elastography for the cornea*. Institut Polytechnique de Paris, Doctoral Thesis (2025). https://doi.org/10.70675/c8a4cfd8z4756z4935z86aaz1638d787c549
11. Badawy, H.A.E., Osman, A., Ahmed, T.A.E., et al. "Evaluation of plant-derived biomaterials for the development of tissue-engineered corneal substitutes", *Journal of Biomedical Materials Research Part A*, 112(12), pp. 2187-2201 (2024). https://doi.org/10.1002/jbm.a.37769
12. Elsheikh, A., Alhasso, D., and Rama, P. "Biomechanical properties of human and porcine corneas", *Experimental Eye Research*, 86(5), pp. 783-790 (2008). https://doi.org/10.1016/j.exer.2008.02.006
13. Zeng, Y., Yang, J., Huang, K., et al. "A comparison of biomechanical properties between human and porcine cornea", *Journal of Biomechanics*, 34(4), pp. 533-537 (2001). https://doi.org/10.1016/S0021-9290(00)00219-0
14. Wang, J., Chen, K., and Kang, G. "A nonlinear fractional viscoelastic constitutive model for time-dependent ratchetting of polyetherimide", *International Journal of Solids and Structures*, 320, Art. 113546 (2025). https://doi.org/10.1016/j.ijsolstr.2025.113546
15. Ilic, D., Moix, T., Lambercy, O., et al. "Measurement of elastic properties of blood vessels", *Proceedings of the 27th Annual International Conference of the IEEE Engineering in Medicine and Biology Society*, pp. 6199-6202 (2005). https://doi.org/10.1109/IEMBS.2005.1615911
16. Nguyen, T.D., Jones, R.E., and Boyce, B.L. "A nonlinear anisotropic viscoelastic model for the tensile behavior of the corneal stroma", *Journal of Biomechanical Engineering*, 130(4), Art. 041020 (2008). https://doi.org/10.1115/1.2947399
17. Mandal, D., Chattopadhyay, H., and Halder, K. "Constitutive modeling of human cornea through fractional calculus approach", *Physics of Fluids*, 35(3), Art. 031907 (2023). https://doi.org/10.1063/5.0138730
18. Das, M., Waeterloos, J.L., Clasen, C., et al. "Single cells are compactly and accurately described as fractional Kelvin-Voigt materials", *Rheologica Acta*, 64(8), pp. 407-421 (2025). https://doi.org/10.1007/s00397-025-01515-w
19. Taheran, F., Ahmadian, M.T., and Firoozbakhsh, K. "Nonlinear oscillations of viscoelastic microcantilever beam based on modified strain gradient theory", *Scientia Iranica*, 28(2), pp. 785-794 (2021). https://doi.org/10.24200/sci.2020.54137.3612
20. Glass, D.H., Roberts, C.J., Litsky, A.S., et al. "A viscoelastic biomechanical model of the cornea describing the effect of viscosity and elasticity on hysteresis", *Investigative Ophthalmology & Visual Science*, 49(9), pp. 3919-3926 (2008). https://doi.org/10.1167/iovs.07-1321
21. Pang, G., Wang, C., Wang, X., et al. "A review of human cornea finite element modeling: geometry modeling, constitutive modeling, and outlooks", *Frontiers in Bioengineering and Biotechnology*, 12, Art. 1455027 (2024). https://doi.org/10.3389/fbioe.2024.1455027
22. Song, D., Lim, S., Park, J., et al. "Linear viscoelasticity of human sclera and posterior ocular tissues during tensile creep", *Journal of Biomechanics*, 151, Art. 111530 (2023). https://doi.org/10.1016/j.jbiomech.2023.111530
23. Lopes, B.T., Bao, F.J., Wang, J.J., et al. "Review of in-vivo characterisation of corneal biomechanics", *Medicine in Novel Technology and Devices*, 11, Art. 100073 (2021). https://doi.org/10.1016/j.medntd.2021.100073
24. Bettahar, T., Rahmoune, C., and Benazzouz, D. "Keratoconus prognosis study for patients with corneal external mechanical stress mode", *International Ophthalmology*, 40(7), pp. 1673-1686 (2020). https://doi.org/10.1007/s10792-020-01335-2
25. Nutting, P.G. "A new general law of deformation", *Journal of the Franklin Institute*, 191(5), pp. 679-685 (1921). https://doi.org/10.1016/S0016-0032(21)90171-6
26. Scott Blair, G.W. "Analytical and integrative aspects of the stress-strain-time problem", *Journal of Scientific Instruments*, 21(5), pp. 80-84 (1944). https://doi.org/10.1088/0950-7671/21/5/302

27. Makris, N. and Constantinou, M.C. “Fractional-derivative Maxwell model for viscous dampers”, *Journal of Structural Engineering*, 117(9), pp. 2708-2724 (1991). https://doi.org/10.1061/(ASCE)0733-9445(1991)117:9(2708)

28. Lewandowski, R. and Chorążyczewski, B. “Identification of the parameters of the Kelvin-Voigt and the Maxwell fractional models, used to modeling of viscoelastic dampers”, *Computers & Structures*, 88(1-2), pp. 1-17 (2010). https://doi.org/10.1016/j.compstruc.2009.09.001

29. Almuneef, A. and Hagag, A.-E. “Approximate solution of the fractional differential equation via the natural decomposition method”, *Revista Internacional de Métodos Numéricos para Cálculo y Diseño en Ingeniería*, 39(4), pp. 1-8 (2023). https://doi.org/10.23967/j.rimni.2023.10.008

30. Tan, W., Pan, W., and Xu, M. “A note on unsteady flows of a viscoelastic fluid with the fractional Maxwell model between two parallel plates”, *International Journal of Non-Linear Mechanics*, 38(5), pp. 645-650 (2003). https://doi.org/10.1016/S0020-7462(01)00121-4

31. Qi, H. and Jin, H. “Unsteady rotating flows of a viscoelastic fluid with the fractional Maxwell model between coaxial cylinders”, *Acta Mechanica Sinica*, 22(4), pp. 301-305 (2006). https://doi.org/10.1007/s10409-006-0013-x

32. Yin, Y. and Zhu, K.-Q. “Oscillating flow of a viscoelastic fluid in a pipe with the fractional Maxwell model”, *Applied Mathematics and Computation*, 173(1), pp. 231-242 (2006). https://doi.org/10.1016/j.amc.2005.04.001

33. Jia, J.-H. and Hua, H.-X. “Study of oscillating flow of viscoelastic fluid with the fractional Maxwell model”, *Journal of Fluids Engineering*, 130(4), Art. 041201 (2008). https://doi.org/10.1115/1.2903517

34. Tripathi, D., Pandey, S.K., and Das, S.K. “Peristaltic flow of viscoelastic fluid with fractional Maxwell model through a channel”, *Applied Mathematics and Computation*, 215(10), pp. 3645-3654 (2010). https://doi.org/10.1016/j.amc.2009.11.002

35. Tripathi, D. “Peristaltic transport of fractional Maxwell fluids in uniform tubes: applications in endoscopy”, *Computers & Mathematics with Applications*, 62(3), pp. 1116-1126 (2011). https://doi.org/10.1016/j.camwa.2011.03.038

36. Nguedjio, L.C., Moutou Pitti, R., Blaysat, B., et al. “Fractional order derivative approach of viscoelastic behavior of tropical wood”, *Proceedings of the 14th World Conference on Timber Engineering*, pp. 5437-5443 (2025). https://doi.org/10.52202/080513-0669

37. Abukhaled, M. and Abukhaled, Y. “Efficient semianalytical investigation of a fractional model describing human cornea shape”, *Modeling and Artificial Intelligence in Ophthalmology*, 6(1), pp. 1-15 (2024). https://doi.org/10.35119/maio.v6i1.138

38. Arif, M.S., Abodayeh, K., and Nawaz, Y. “Explicit computational analysis of unsteady Maxwell nanofluid flow on moving plates with stochastic variations”, *International Journal of Thermofluids*, 23, Art. 100755 (2024). https://doi.org/10.1016/j.ijft.2024.100755

39. Ciancio, A., Ciancio, V., and Flora, B.F.F. “A fractional rheological model of viscoelastic media”, *Axioms*, 12(3), Art. 243 (2023). https://doi.org/10.3390/axioms12030243

40. Zheng, J. and Jian, Y. “Transient rotating magnetohydrodynamic electroosmotic flow using time-fractional Caputo-Fabrizio derivative”, *Physics of Fluids*, 37(2), Art. 022021 (2025). https://doi.org/10.1063/5.0254733

41. Bonifasi-Lista, C., Lake, S.P., Small, M.S., et al. “Viscoelastic properties of the human medial collateral ligament under longitudinal, transverse and shear loading”, *Journal of Orthopaedic Research*, 23(1), pp. 67-76 (2005). https://doi.org/10.1016/j.orthres.2004.06.002

42. Shah, S.H.A.M. and Qi, H. “Starting solutions for a viscoelastic fluid with fractional Burgers model in an annular pipe”, *Nonlinear Analysis: Real World Applications*, 11(1), pp. 547-554 (2010). https://doi.org/10.1016/j.nonrwa.2009.01.012

43. Friedrich, C. “Relaxation and retardation functions of the Maxwell model with fractional derivatives”, *Rheologica Acta*, 30(2), pp. 151-158 (1991). https://doi.org/10.1007/BF01134604

44. Yang, G., Zhao, H., Hu, Z., et al. “Prediction of restrained stress for UHPC: considering relationship between long-term and in-situ creep”, *Construction and Building Materials*, 484, Art. 141722 (2025). https://doi.org/10.1016/j.conbuildmat.2025.141722

45. Yang, G., Cao, Q., Zhao, H., et al. “New insights into linear-nonlinear tensile creep mechanisms of UHPC: stress level-dependent creep-active site transitions”, *Cement and Concrete Research*, 198, Art. 107988 (2025). https://doi.org/10.1016/j.cemconres.2025.107988

46. Zhang, C., Lou, M., Wang, Y., et al. “Mechanical responses and microscopic irreversible deformation evolution of thermoplastic fiber-reinforced composites under cyclic loading”, *International Journal of Fatigue*, 203, Art. 109327 (2026). https://doi.org/10.1016/j.ijfatigue.2025.109327

47. Zou, D., Liu, G., Rao, Z., et al. “A device capable of customizing nonlinear forces for vibration energy harvesting, vibration isolation, and nonlinear energy sink”, *Mechanical Systems and Signal Processing*, 147, Art. 107101 (2021). https://doi.org/10.1016/j.ymssp.2020.107101

48. Wang, Q., Zhong, L., Zhou, Y., et al. “Hierarchical cellulose nanopaper origami electronics”, *Carbohydrate Polymers*, 373, Art. 124627 (2026). https://doi.org/10.1016/j.carbpol.2025.124627

49. Meyers, M.A. and Chawla, K.K. *Mechanical Behavior of Materials*. Cambridge University Press, 2nd ed. (2008). https://www.cambridge.org/highereducation/books/mechanical-behavior-of-materials/48AD6E15E989D76D5DAF9926123137CF

50. He, J.-H. “A remark on “A nonlinear mathematical model of the corneal shape””, *Nonlinear Analysis: Real World Applications*, 13(6), pp. 2863-2865 (2012). https://doi.org/10.1016/j.nonrwa.2012.02.020

51. Cheng, A.H.-D., Sidauruk, P., and Abousleiman, Y. “Approximate inversion of the Laplace transform”, *The Mathematica Journal*, 4(2), pp. 76-82 (1994). https://library.wolfram.com/infocenter/Articles/1516/

52. Erturk, V.S., Ahmadkhanlu, A., Kumar, P., et al. "Some novel mathematical analysis on a corneal shape model by using Caputo fractional derivative", *Optik*, 261, Art. 169086 (2022). https://doi.org/10.1016/j.ijleo.2022.169086

53. Guo, J., Yin, Y., Hu, X., et al. "Self-similar network model for fractional-order neuronal spiking: implications of dendritic spine functions", *Nonlinear Dynamics*, 100(1), pp. 921-935 (2020). https://doi.org/10.1007/s11071-020-05519-4

Biographies

Mohammadnabi Farrahi is a mechanical engineering researcher at Babol Noshirvani University of Technology, Babol, Iran. His research interests include biomechanical modeling, viscoelasticity, fractional-order constitutive modeling, computational mechanics, and numerical simulation of soft biological tissues. His current work focuses on combining fractional calculus with Laplace-domain solution techniques to characterize creep and stress-relaxation responses in the human cornea. He has experience with MATLAB-based numerical analysis and finite-element validation using Abaqus.

Davood Domiri Ganji is a professor of mechanical engineering at Babol Noshirvani University of Technology, Babol, Iran. His research covers nonlinear differential equations, analytical and semi-analytical solution methods, fluid mechanics, heat transfer, nonlinear dynamics, and computational biomechanics. He has supervised research on mathematical modeling of complex engineering systems and has contributed extensively to the development and application of methods for nonlinear ordinary and partial differential equations. In the present study, his expertise supports the formulation, analysis, and validation of the fractional Maxwell model for corneal tissue. His work emphasizes efficient mathematical methods and their practical application to multidisciplinary problems in mechanics and engineering.

Payam Jalili is a faculty member in mechanical engineering at the North Tehran Branch of Islamic Azad University, Tehran, Iran, and he is head of Research Center for Modern Energy Technologies. His research interests include nonlinear dynamics, computational mechanics, renewable energy systems, artificial intelligence applications in engineering, vibration analysis, and mathematical modeling. He has contributed to studies that combine analytical, numerical, and data-driven methods for the investigation of complex mechanical and energy systems. In this work, he contributes to the interpretation and computational analysis of fractional-order viscoelastic behavior, with particular attention to the predictive modeling of creep and stress relaxation in corneal tissue.

List of Figure Captions

Fig. 1. Maxwell model.

Fig. 2. Creep-recovery response of the Maxwell model.

Fig. 3. (a) Elastic element, (b) viscous element, and (c) fractional element.

Fig. 4. Schematic representation of (a) the classical Maxwell model and (b) the fractional Maxwell model.

Fig. 5. Comparison of the numerically inverted function with the analytical result.

Fig. 6. Boundary conditions for (a) the creep test and (b) the stress-relaxation test.

Fig. 7. Comparison of creep responses predicted by the classical Maxwell model and Abaqus.

Fig. 8. Comparison of stress-relaxation responses predicted by the classical Maxwell model and Abaqus.

Fig. 9. Stress-strain responses for different β values compared with experimental data at (a) $\alpha = 0.2$, (b) $\alpha = 0.4$, (c) $\alpha = 0.5$, (d) $\alpha = 0.6$, (e) $\alpha = 0.8$, and (f) $\alpha = 1.0$.

Fig. 10. Comparison of experimental stress-strain data with the classical Maxwell model and the present fractional model.

Fig. 11. Comparison of stress-relaxation responses from Abaqus, the classical Maxwell model, and the present fractional model.

Fig. 12. Comparison of creep responses from Abaqus, the classical Maxwell model, and the present fractional model.

Fig. 13. Sensitivity of stress relaxation to β at fixed α: (a) $\alpha = 0.2$, (b) $\alpha = 0.4$, (c) $\alpha = 0.5$, (d) $\alpha = 0.6$, (e) $\alpha = 0.8$, and (f) $\alpha = 1.0$.

Fig. 14. Sensitivity of stress relaxation to α at fixed β: (a) $\beta = 0.2$, (b) $\beta = 0.4$, (c) $\beta = 0.5$, (d) $\beta = 0.6$, (e) $\beta = 0.8$, and (f) $\beta = 1.0$.

Fig. 15. Sensitivity of creep to β at fixed α: (a) $\alpha = 0.2$, (b) $\alpha = 0.4$, (c) $\alpha = 0.5$, (d) $\alpha = 0.6$, (e) $\alpha = 0.8$, and (f) $\alpha = 1.0$.

Fig. 16. Sensitivity of creep to α at fixed β: (a) $\beta = 0.2$, (b) $\beta = 0.4$, (c) $\beta = 0.5$, (d) $\beta = 0.6$, (e) $\beta = 0.8$, and (f) $\beta = 1.0$.

List of Table Captions

Table 1. Computational procedure of the Gaver-Stehfest inversion method.

Table 2. Fractional parameter values used in the simulations.

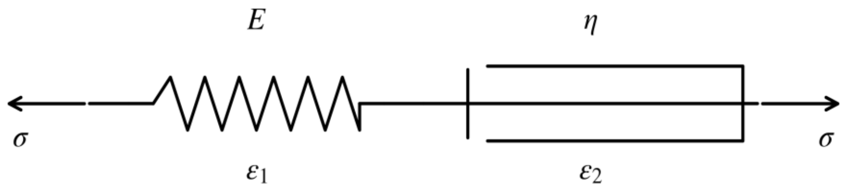

Fig. 1. Maxwell model.

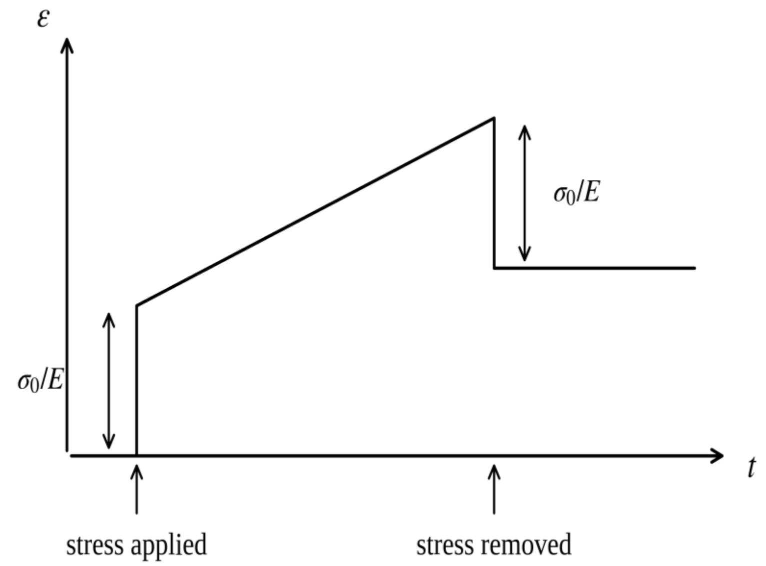

Fig. 2. Creep-recovery response of the Maxwell model.

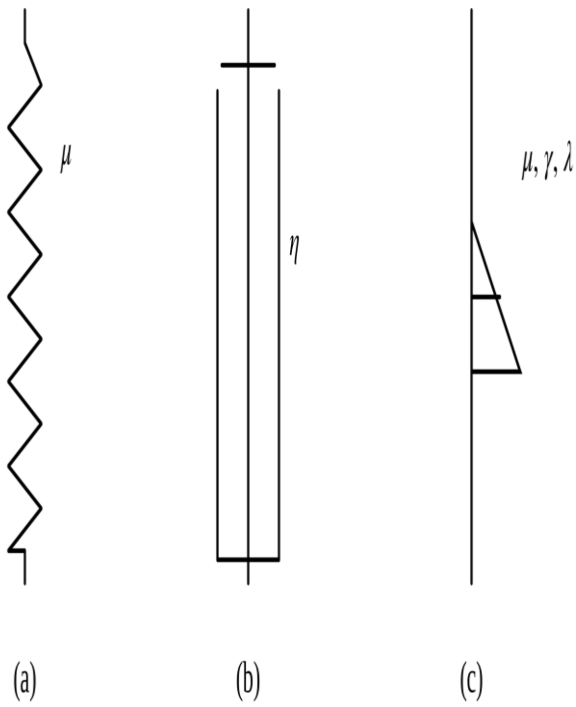

Fig. 3. (a) Elastic element, (b) viscous element, and (c) fractional element.

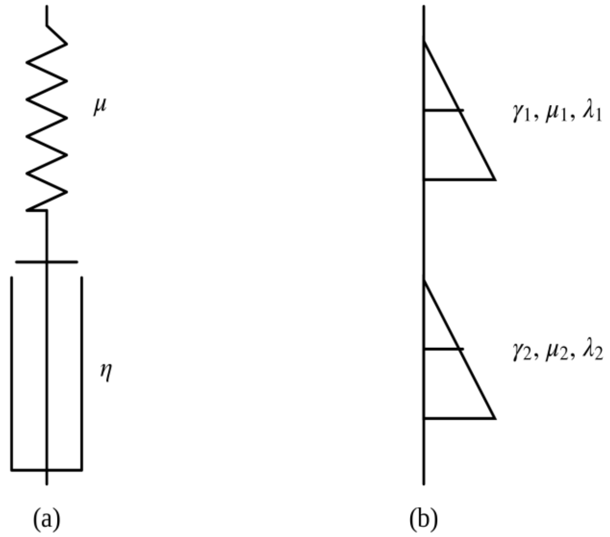

Fig. 4. Schematic representation of (a) the classical Maxwell model and (b) the fractional Maxwell model.

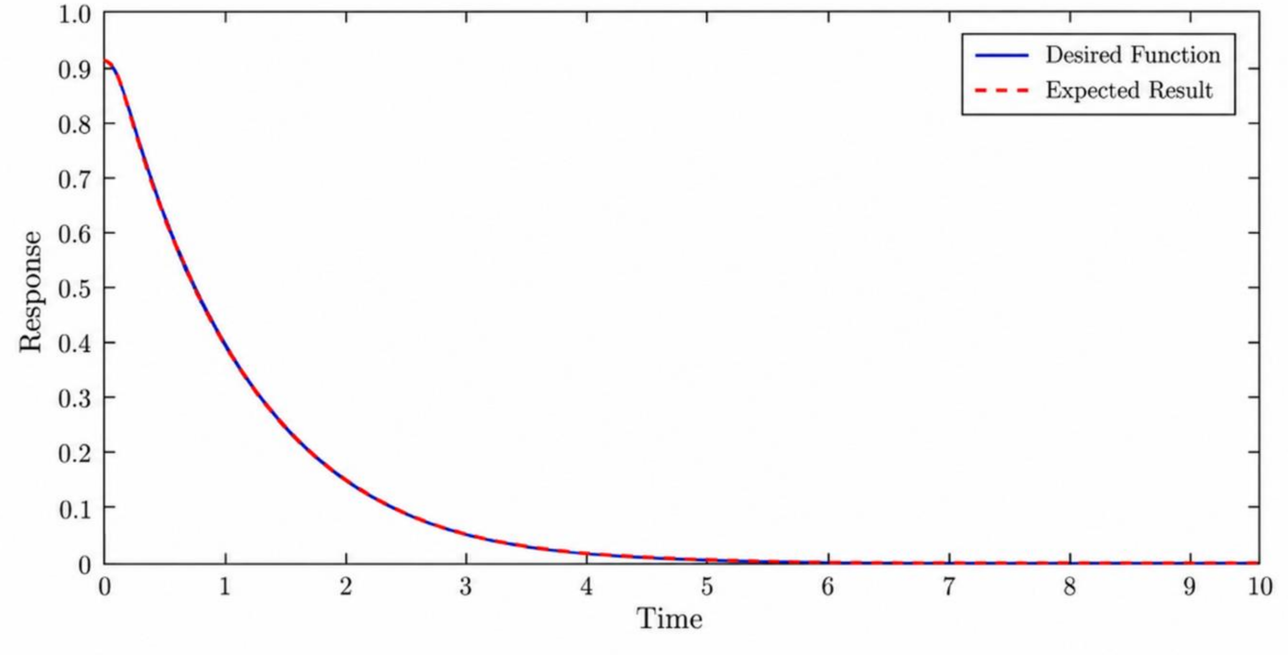

Fig. 5. Comparison of the numerically inverted function with the analytical result.

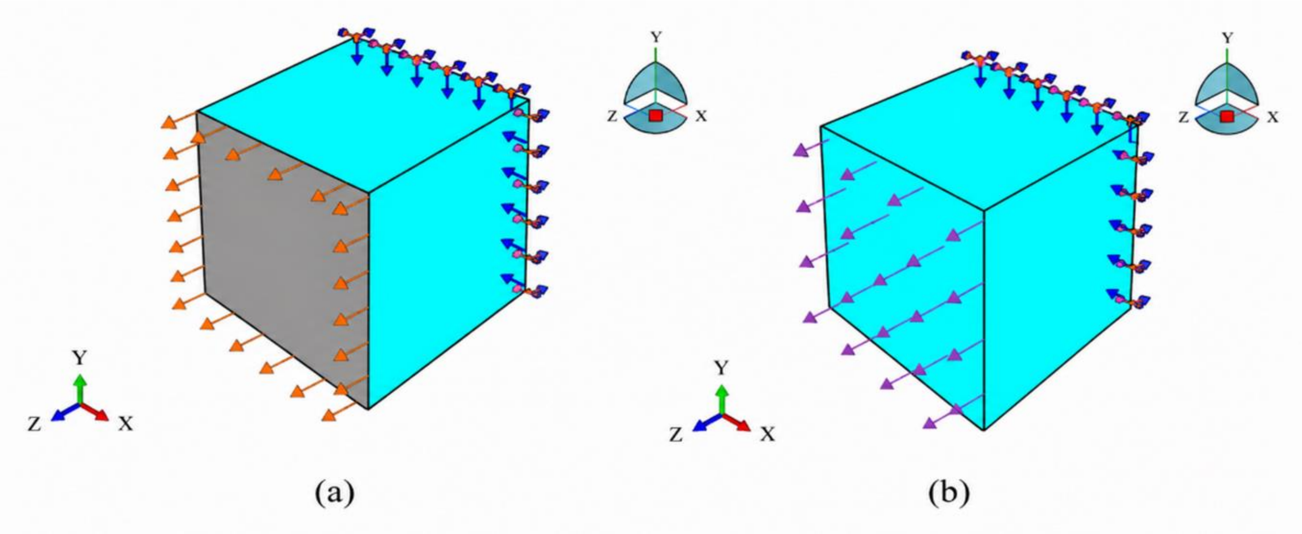

Fig. 6. Boundary conditions for (a) the creep test and (b) the stress-relaxation test.

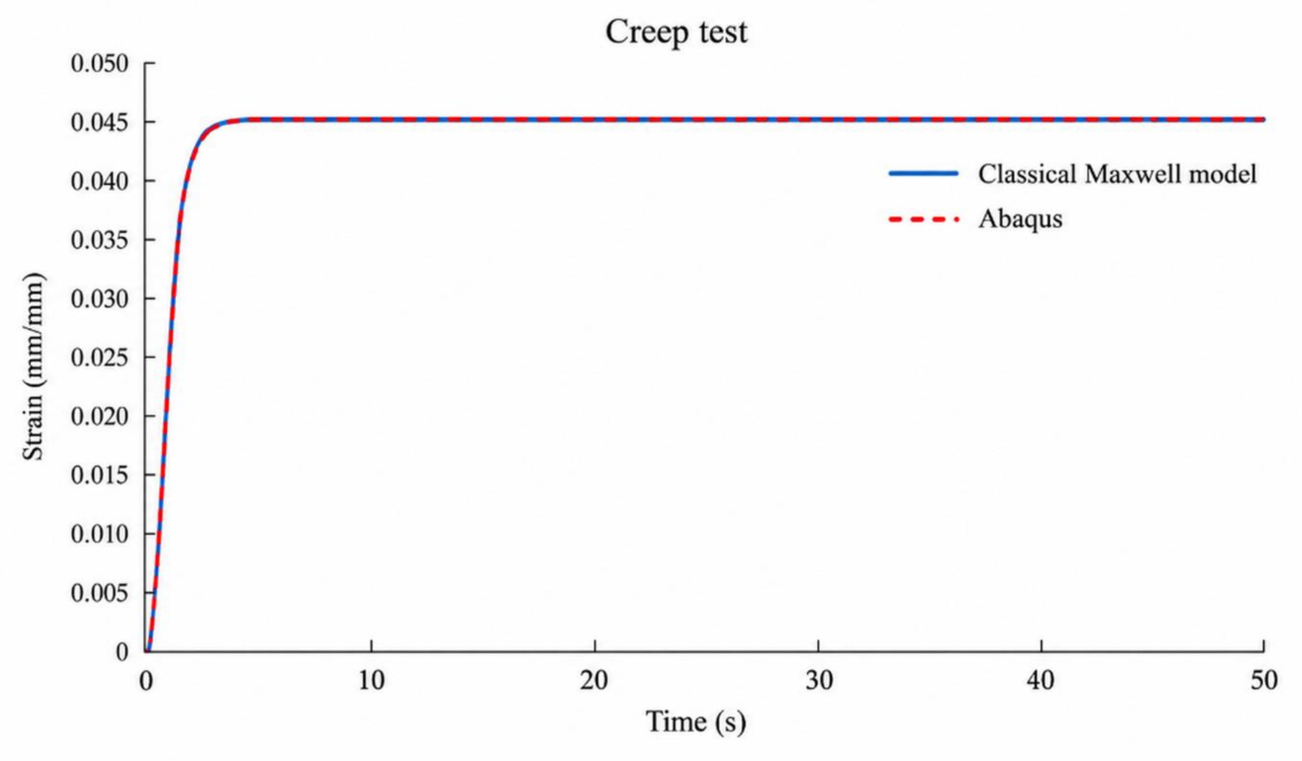

Fig. 7. Comparison of creep responses predicted by the classical Maxwell model and Abaqus.

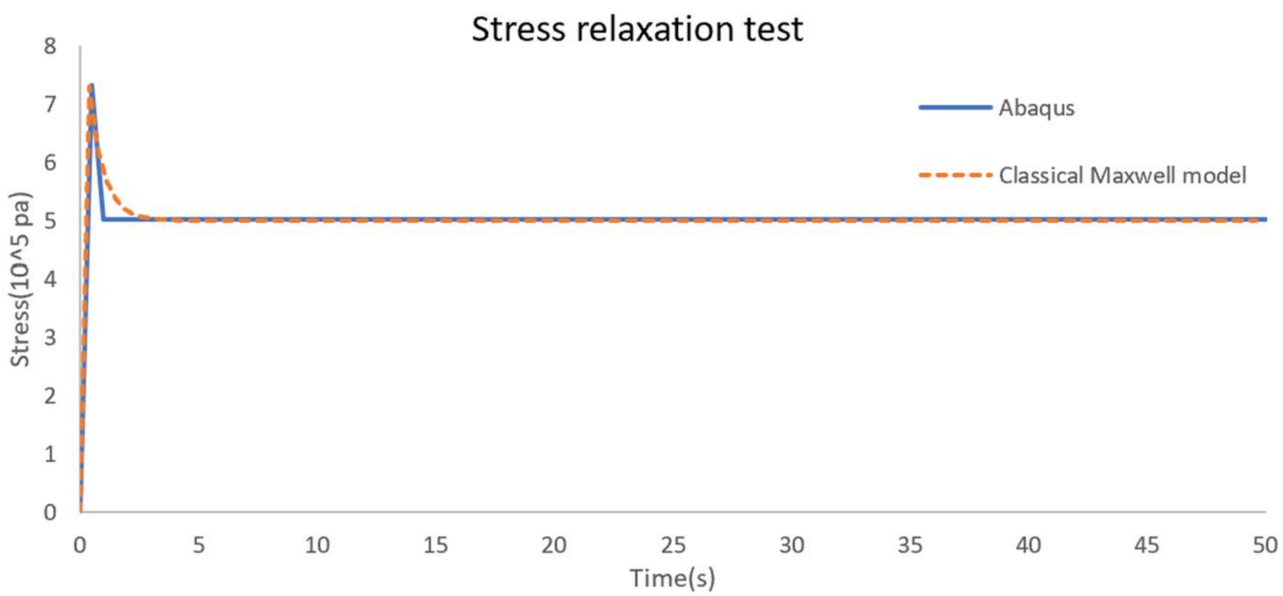

Fig. 8. Comparison of stress-relaxation responses predicted by the classical Maxwell model and Abaqus.

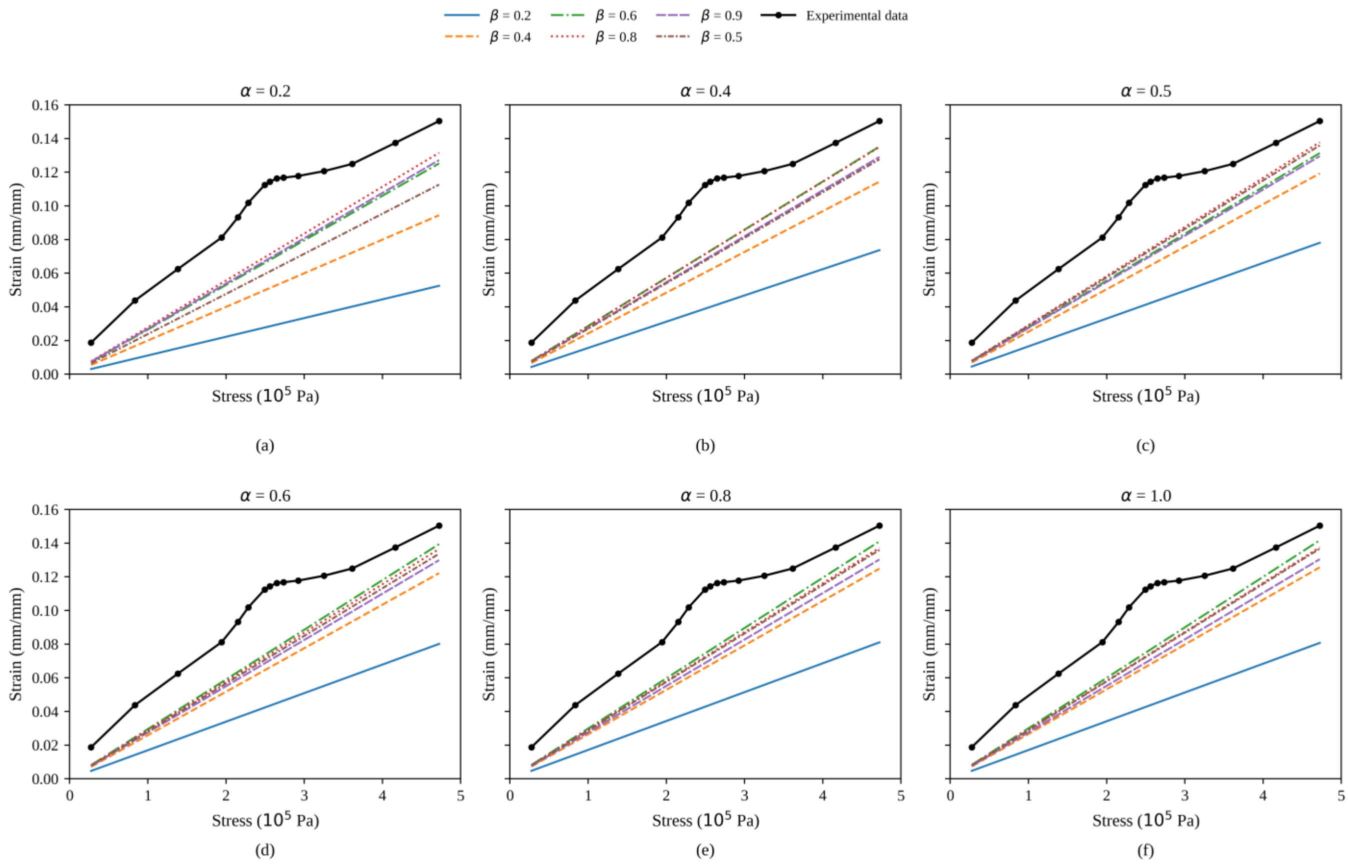

Fig. 9. Stress-strain responses for different β values compared with experimental data at (a) α = 0.2, (b) α = 0.4, (c) α = 0.5, (d) α = 0.6, (e) α = 0.8, and (f) α = 1.0.

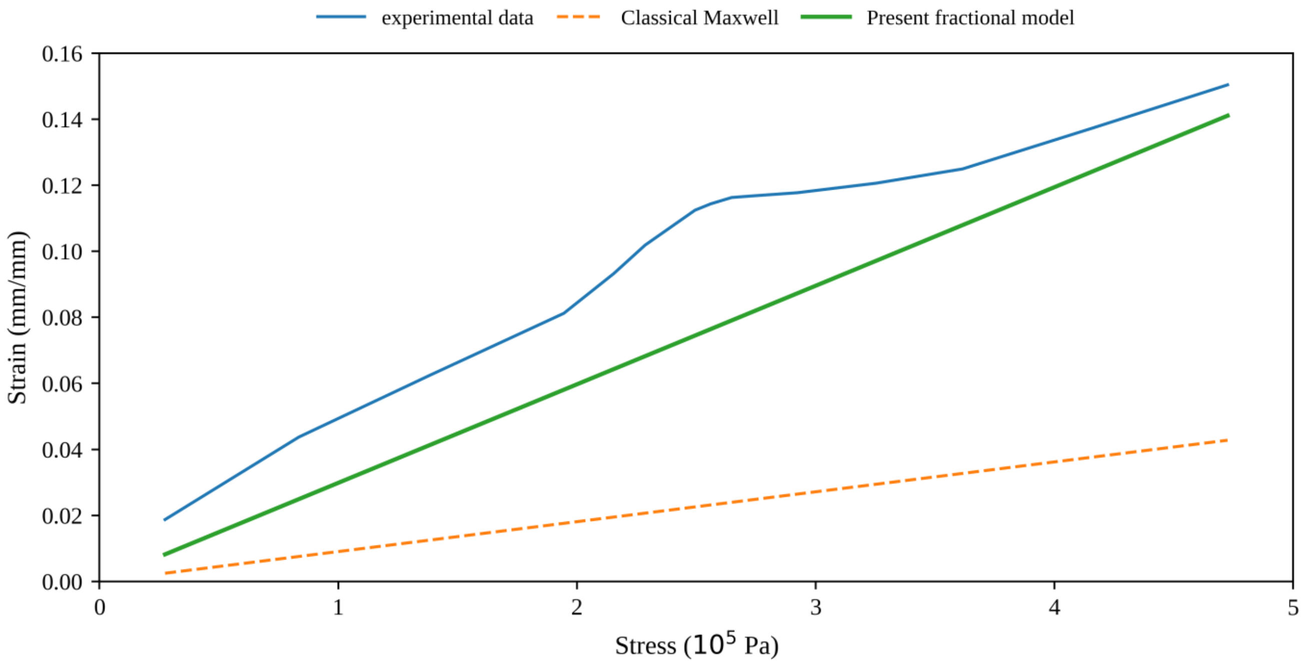

Fig. 10. Comparison of experimental stress-strain data with the classical Maxwell model and the present fractional model.

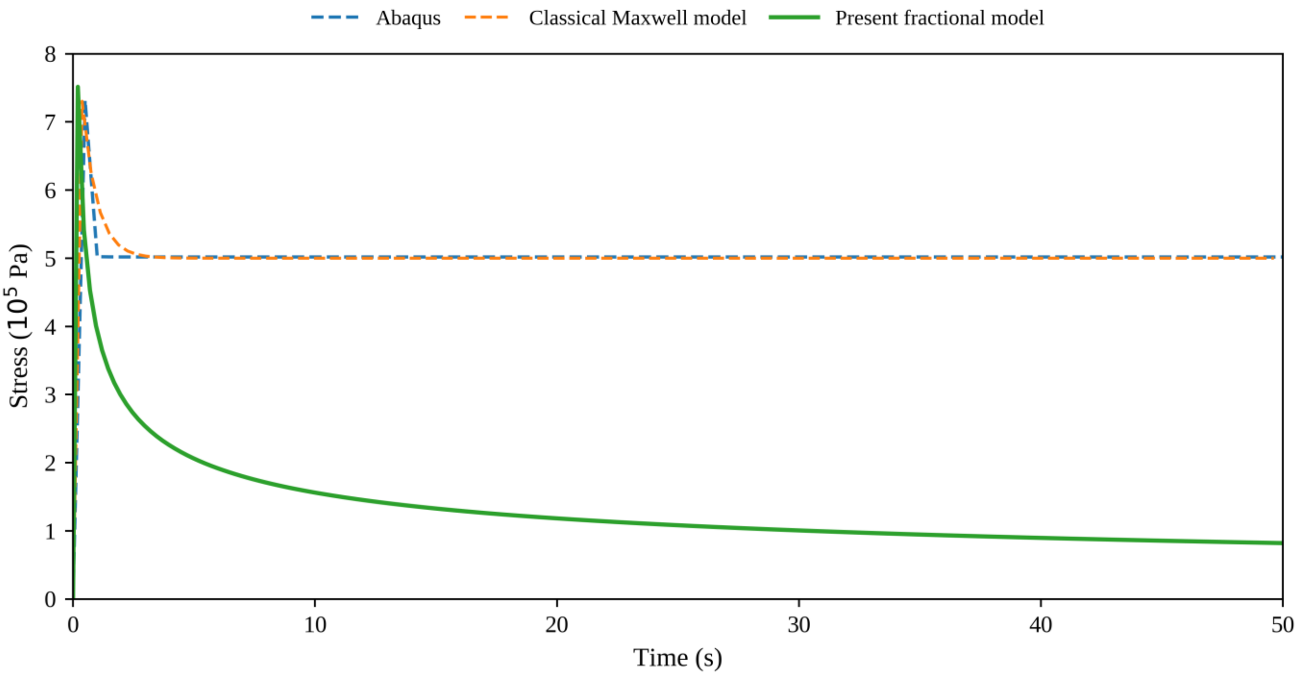

Fig. 11. Comparison of stress-relaxation responses from Abaqus, the classical Maxwell model, and the present fractional model.

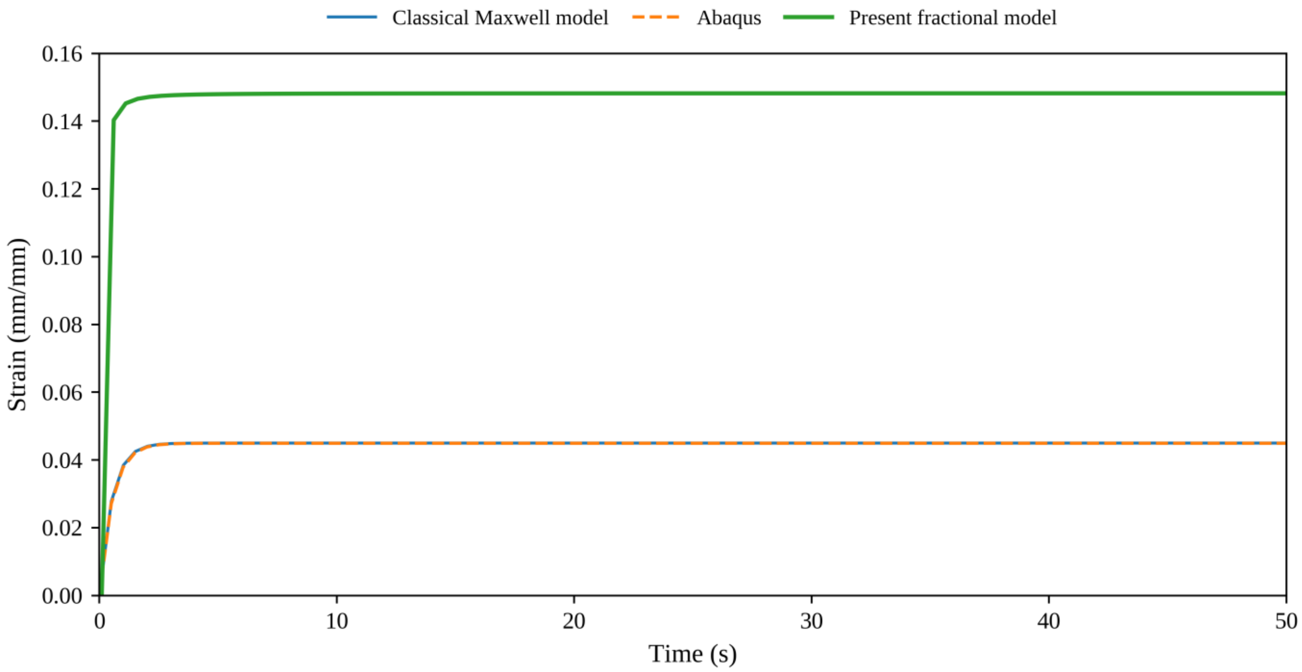

Fig. 12. Comparison of creep responses from Abaqus, the classical Maxwell model, and the present fractional model.

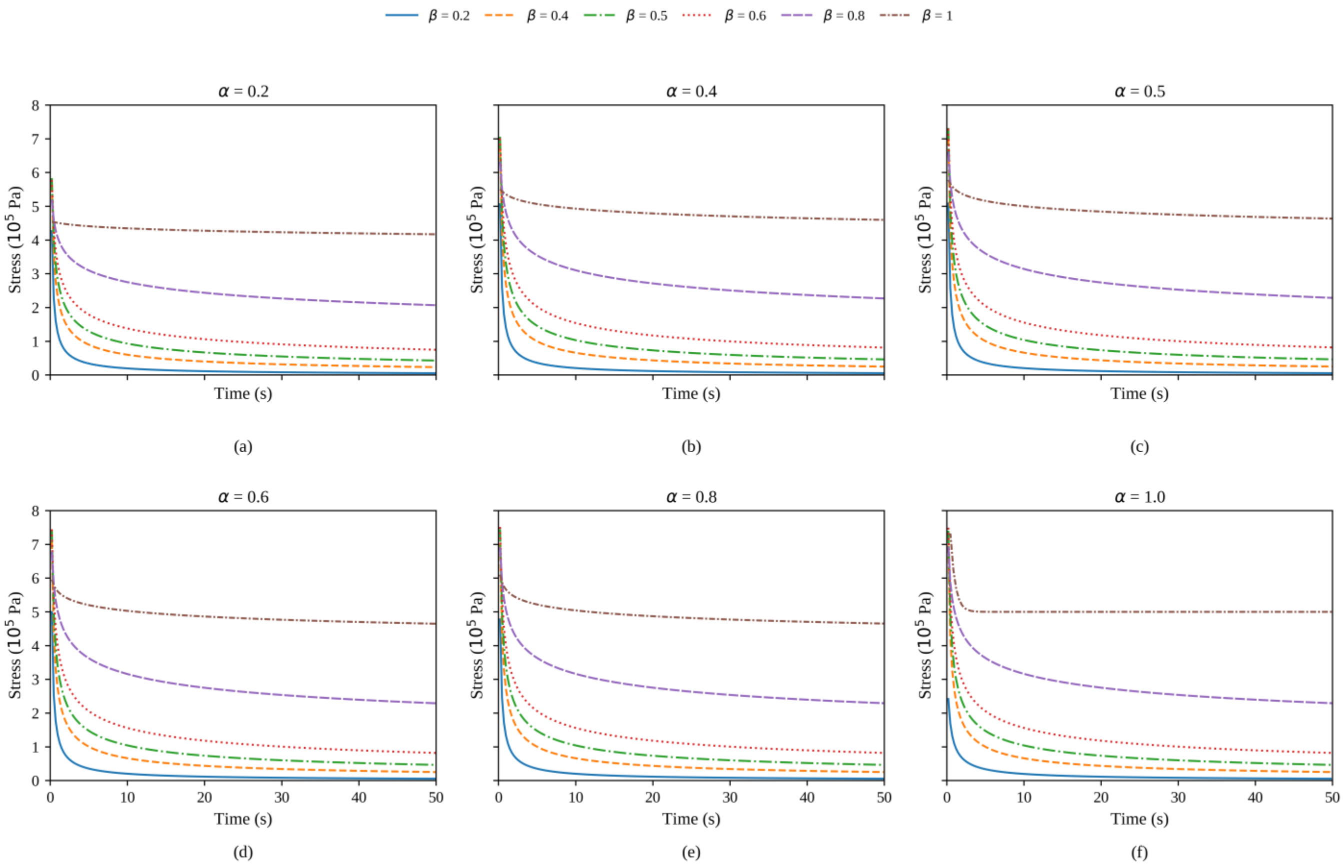

Fig. 13. Sensitivity of stress relaxation to β at fixed α: (a) α = 0.2, (b) α = 0.4, (c) α = 0.5, (d) α = 0.6, (e) α = 0.8, and (f) α = 1.0.

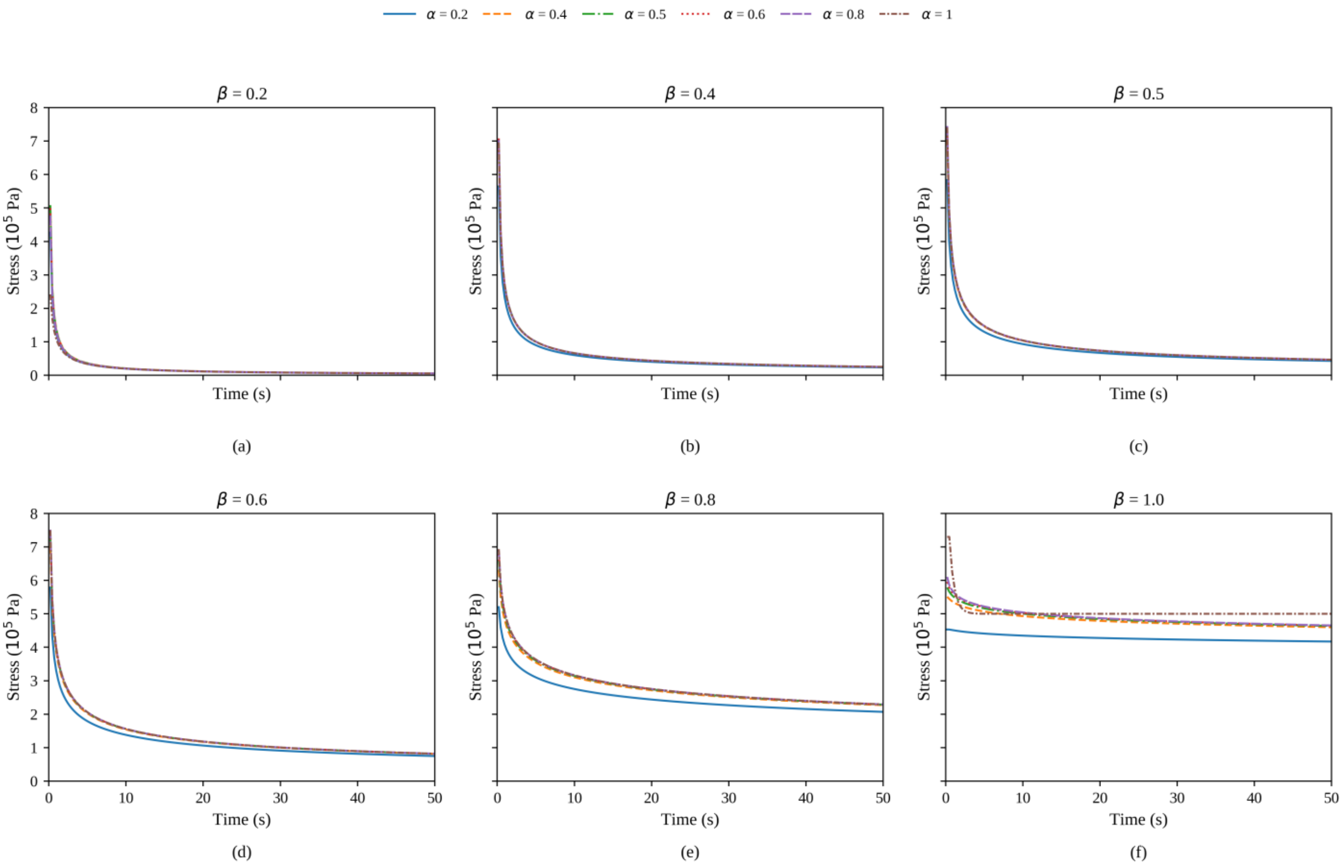

Fig. 14. Sensitivity of stress relaxation to α at fixed β: (a) β = 0.2, (b) β = 0.4, (c) β = 0.5, (d) β = 0.6, (e) β = 0.8, and (f) β = 1.0.

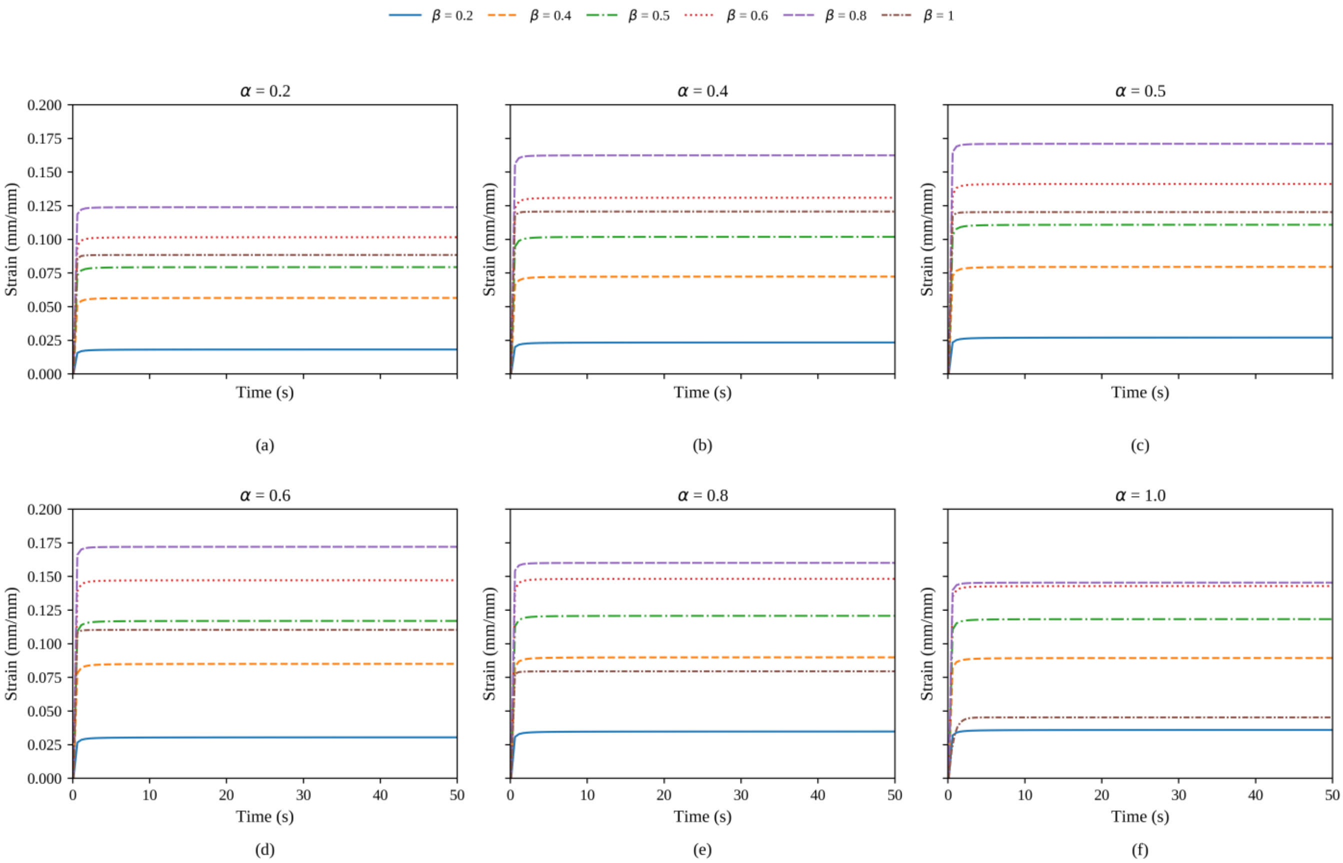

Fig. 15. Sensitivity of creep to β at fixed α: (a) α = 0.2, (b) α = 0.4, (c) α = 0.5, (d) α = 0.6, (e) α = 0.8, and (f) α = 1.0.

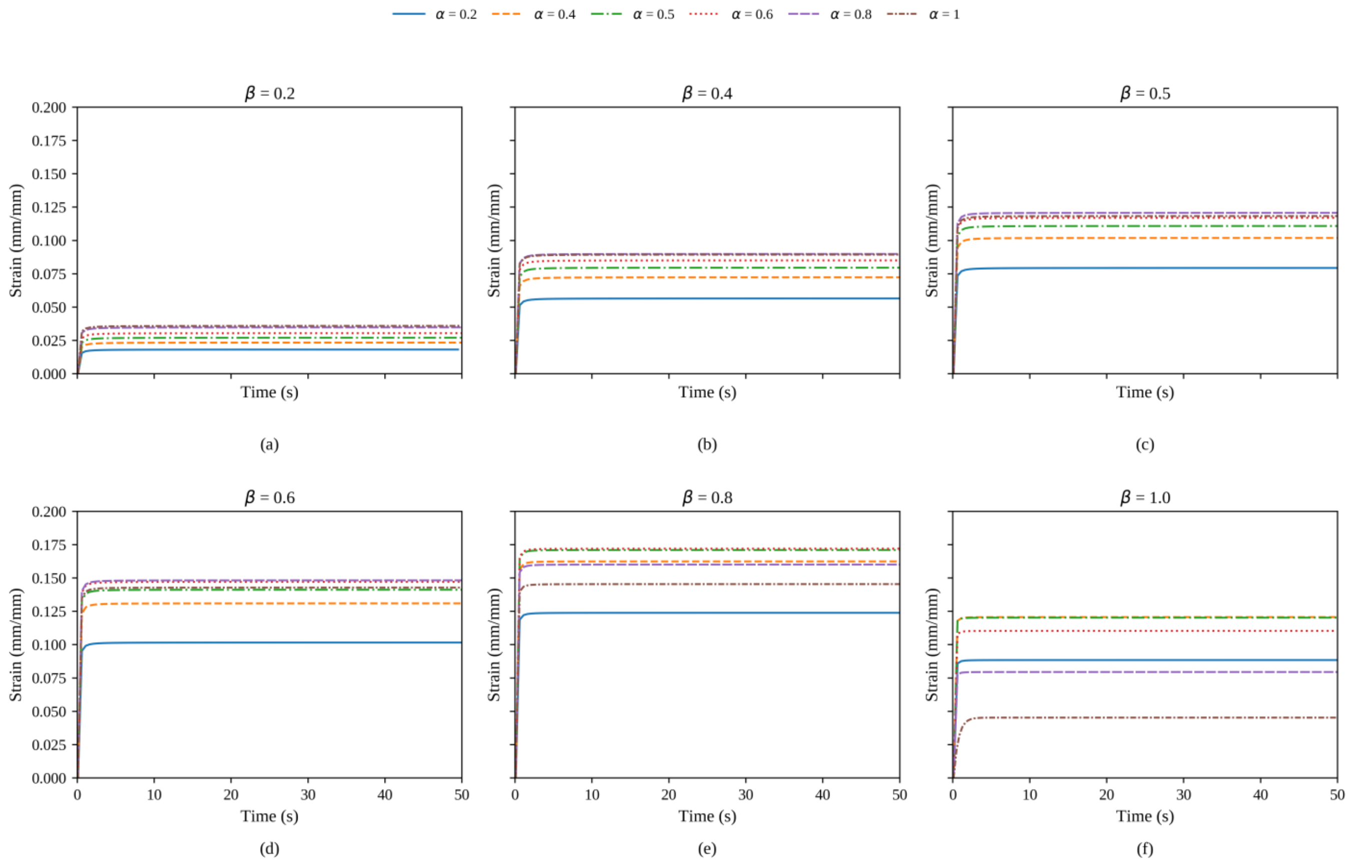

Fig. 16. Sensitivity of creep to α at fixed β: (a) β = 0.2, (b) β = 0.4, (c) β = 0.5, (d) β = 0.6, (e) β = 0.8, and (f) β = 1.0.

Tables

Table 1. Computational procedure of the Gaver-Stehfest inversion method.

Step	Procedure
1	Define the constitutive model, σ(s) or ε(s), in the Laplace domain.
2	Apply the Laplace transform to the fractional Maxwell equation.
3	Substitute the fractional parameters α and β and obtain F(s) = L{f(t)}.
4	For a selected even value of N, compute the Stehfest weighting coefficients V_k.
5	For k = 1, 2, …, N, evaluate F(k ln(2)/t).
6	Compute $f(t) = [\ln(2)/t]\ \Sigma_{k=1}^{N}\ V_k F[k \ln(2)/t]$.
7	Obtain the time-domain creep or stress-relaxation response.

Table 2. Fractional parameter values used in the simulations.

Parameter	Values
α	0.2, 0.4, 0.5, 0.6, 0.8, 1.0
β	0.2, 0.4, 0.5, 0.6, 0.8, 1.0